

Stochastic resonance in thermally activated reactions: Application to biological ion channels

Sergey M. Bezrukov^{a)}

Laboratory of Physical and Structural Biology, NICHD, National Institutes of Health, Bethesda, Maryland 20892-0924 and St. Petersburg Nuclear Physics Institute, Gatchina, Russia 188350

Igor Vodyanoy

Laboratory of Physical and Structural Biology, NICHD, National Institutes of Health, Bethesda, Maryland 20892-0924 and Office of Naval Research, Europe, 223 Old Marylebone Road, London, NW1 5TH, United Kingdom

(Received 21 January 1998; accepted for publication 28 April 1998)

At the molecular level many thermally activated reactions can be viewed as Poisson trains of events whose instantaneous rates are defined by the reaction activation barrier height and an effective collision frequency. When the barrier height depends on an external parameter, variation in this parameter induces variation in the event rate. Extending our previous work, we offer a detailed theoretical analysis of signal transduction properties of these reactions considering the external parameter as an input signal and the train of resulting events as an output signal. The addition of noise to the system input facilitates signal transduction in two ways. First, for a linear relationship between the barrier height and the external parameter the output signal power grows exponentially with the mean square fluctuation of the noise. Second, for noise of a sufficiently high bandwidth, its addition increases output signal quality measured as the signal-to-noise ratio (SNR). The output SNR reaches a maximum at optimal noise intensity defined by the reaction sensitivity to the external parameter, reaction initial rate, and the noise bandwidth. We apply this theory to ion channels of excitable biological membranes. Based on classical results of Hodgkin and Huxley we show that open/closed transitions of voltage-gated ion channels can be treated as thermally activated reactions whose activation barriers change linearly with applied transmembrane voltage. As an experimental example we discuss our recent results obtained with polypeptide alamethicin incorporated into planar lipid bilayers. © 1998 American Institute of Physics. [S1054-1500(98)01303-2]

“Stochastic Resonance” (SR), a phenomenon of noise-facilitated signal transduction,¹ has been previously reported for a variety of *macroscopic* systems, however, it is now found experimentally and explained theoretically at the *microscopic* level—the level of thermally activated molecular reactions. We analyze a time-dependent (“doubly stochastic”²) Poisson process where the event generation rate is an exponential function of an external parameter. Recently we have shown³ that this process exhibits SR representing nondynamical threshold-free systems that are able to transfer small signals with a finite, signal-amplitude-independent transduction coefficient. Thus, we have found that SR is an inherent property of a wide variety of systems described by general reaction rate models that range from voltage-gated ion channels of biological membranes to p-n semiconductor structures. Here we present a detailed analysis of the influence of a filtered “white” Gaussian noise on the signal transduction in these systems, examining the output signal amplitude and signal-to-noise ratio (SNR) as functions of input noise parameters. Also, using the classical results of Hodgkin and Huxley,⁴ we show that ion channel conformational dynamics can be formally regarded as thermally activated reactions. Finally, we relate tradi-

tional parameters employed in the electrophysiology of ion channels of excitable membranes to those used in the general rate theory.^{5,6}

I. INTRODUCTION

Previous theoretical and experimental studies of the role of external (ambient) noise in electrical signal transduction in biology have been mostly addressing rather complex objects starting from neurons,^{7–11} neuronal ensembles,^{12,13} isolated sciatic nerves of a toad,^{14,15} rat SA1 cutaneous mechanoreceptors,¹⁶ mechanosensory transduction pathways in arthropods,^{17,18} and up to complicated systems of human sensory perception.^{19–22} For all these objects the addition of noise to the system input increased output signal detectability whenever noise characteristics were chosen in a proper way dictated by the system properties.

It is widely recognized that voltage-gated ion channels are critical elements of signal transduction at several levels of biological complexity. In addition to the classical illustrations such as nerve action potential generation²³ and synaptic transmission,²⁴ current research reveals examples of the ion channel crucial role in small electrical signal detection. In a careful study of electroreceptive organs of *Elasmobranch* fish called *ampulae* of Lorenzini it was shown that the ampullary epithelium acts as a linear amplifier of small electric

^{a)}Electronic mail: bezrukov@helix.nih.gov

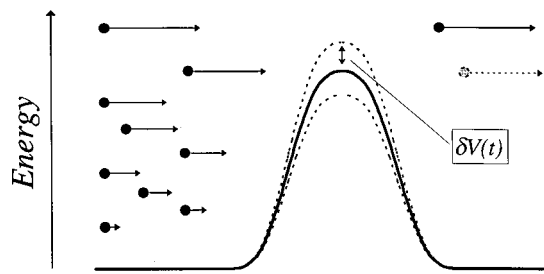


FIG. 1. Schematic illustration of a mechanism for generation of the time-dependent Poisson process. Particles randomly distributed in space and energy attempt to overcome a barrier with the time-dependent height. An “event” is generated every time a particle crosses the barrier. A decreased barrier height will correspond to a higher event rate. If particles are emitted with an exponential distribution in energy, the process is modulated in such a way that the instantaneous rate is proportional to $\exp(-\beta V(t))$.

fields.²⁵ “*In vitro*” measurements performed on a single isolated organ demonstrated a reliable change in the spike firing rate of the afferent nerve for holding potential differences as small as 3×10^{-6} V. Due to the organ’s relative simplicity, this remarkable sensitivity was attributed to voltage-gated ion channels of apical and basal membranes of the receptor cell.

Studies with alamethicin ion channels incorporated into planar lipid membranes^{26,27} showed that the addition of voltage noise to the membrane holding potential facilitates signal transduction in this system. Though significantly different from voltage-gated channels of biological membranes by their structure and by the mechanism of their voltage dependence, alamethicin channels are surprisingly close to sodium channels of nerve membrane by the main parameter characterizing channel sensitivity to transmembrane electric field—the so-called “equivalent voltage sensitivity.” Thus, results obtained with the model peptide channel-former, alamethicin, suggest that the ambient noise utilization is possible already at the membrane level. In the present paper we show that the conformational transitions of voltage-gated biological channels between their open and closed states can be viewed as a thermally activated reaction. We discuss signal transduction properties of such reactions in the presence of additive input noise.

II. SIGNAL TRANSDUCTION IN THERMALLY ACTIVATED REACTIONS

The Van’t Hoff-Arrhenius law, empirically relating escape rate r with the reaction activation energy E_b ,

$$r = \nu \exp(-E_b/kT), \quad (1)$$

where k and T have their regular meaning and ν is a temperature-independent coefficient, has been known for more than a century. It is a very universal relation that covers a wide range of various phenomena in physics, chemistry, and biology. The nature of this universality is well understood—different models of the reaction-rate theory give a particle escape rate that is an exponential or nearly exponential function of the activation barrier height (for reviews see Refs. 5,6).

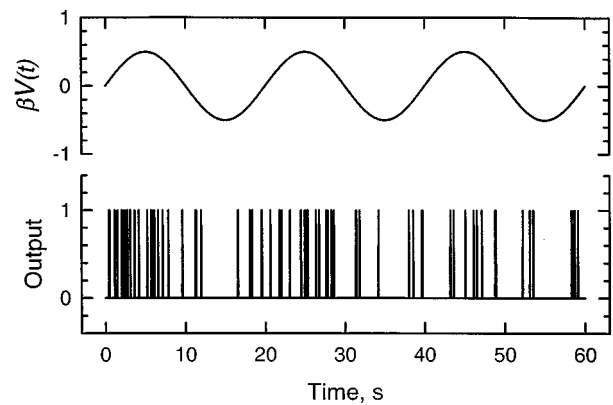


FIG. 2. Example of a time-dependent Poisson train of identical short pulses (lower trace) in the presence of a periodic modulation. A slow (0.05 Hz) sine-wave signal changes the barrier height with the dimensionless amplitude of 0.5. In this simulation the initial undisturbed rate, that is, the rate corresponding to $V(t)=0$, is chosen to be equal to one pulse per second. Rate modulation of the output is seen as the dilution of pulse density during negative half-waves and the concentration of pulse density during positive half-waves.

Reaction rates of many processes are controlled by activation barriers whose heights dependence on an external parameter, e.g., voltage $V(t)$, is close to linear. In this case Eq. (1) can be written in the form

$$r(V(t)) = r(0) \exp(\beta V(t)), \quad (2)$$

where $r(0)$ is the initial process rate and β is the reaction sensitivity to the external parameter.

A mechanism for the Poisson process generated according to Eq. (2) can be illustrated as shown in Figure 1. A stationary beam of particles emitted with an exponential distribution of kinetic energies encounters a barrier whose height depends on an external parameter. An output event, e.g., a short electrical current pulse, is generated every time a particle crosses the barrier. If barrier energy variation is a linear function of the external parameter and particles are spatially uncorrelated, the output process is a time-dependent Poisson train of pulses with the instant rate controlled by the external parameter that we regard as a system input. It is clear that for small input signals, that is for small variations in the external parameter, the relation between the input signal and the output pulse rate is linear. Thus, the system is a linear transducer of small signals with a finite, signal-amplitude-independent coefficient.

Figure 2 shows a computer-simulated output Poisson process (lower trace) whose rate is modulated by a sine-wave input signal (upper trace). The output is a train of uniform randomly generated pulses with information about the input signal encoded in statistical properties of pulse arrival times. Pulse density correlates with the signal and is clearly higher for its positive half-waves than it is for the negative ones. The output signal component can be recovered by many methods, the most common being optimal filtering.²⁸

The time-dependent Poisson process described above can be viewed as random sampling of the signal-modulated barrier height by the oncoming particles (Figure 1). It is clear that the signal transduction quality can be improved by in-

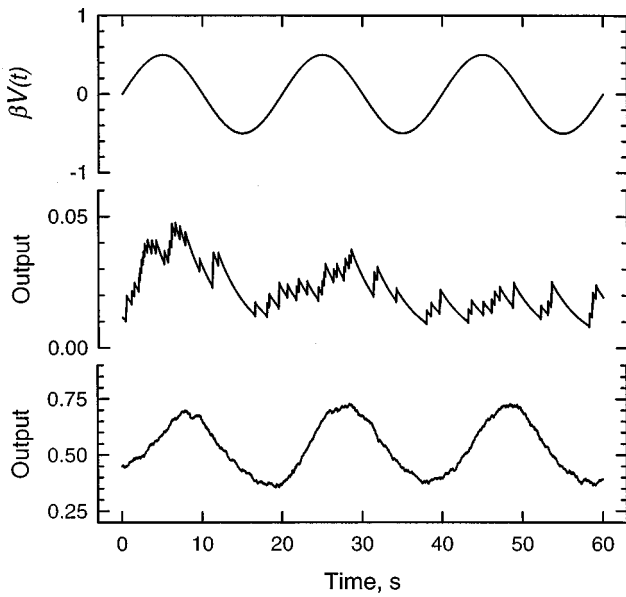


FIG. 3. Increased statistics help signal detection. A filtered pulse output of Figure 2 shows the sine-wave signal contaminated by noise stemming from the randomness of pulse arrival times (*middle trace*). Similarly a generated pulse train with a 25-fold higher statistics (*bottom trace*—initial rate of 25 pulses per second) reveals a higher quality signal. In nonlinear systems represented by Eq. (2), statistics, and, therefore, output signal quality, can be increased by the addition of noise to the system input.

creasing statistics. The signal-to-noise ratio (SNR) at the system output has to increase with the initial rate, $r(0)$, increasing. Indeed, general considerations show that the output signal amplitude is proportional to $r(0)$, while noise amplitude grows only as a square root from the number of events and, for that reason, is proportional to $\sqrt{r(0)}$. This point is illustrated by Figure 3, which compares two output signals with the 25-fold differing statistics. A dramatic increase in signal transduction quality is readily seen in the lower track corresponding to higher $r(0)$.

The relation between the Poisson process rate and the input signal given by Eq. (2) is superlinear. It means that a random zero-mean voltage applied to the system input will increase the average process rate. If noise is added to a signal, this noise-induced increase in statistics could increase signal transduction quality the way it is illustrated by Figure 3. However, the complication is that the added noise will be transduced to the system output by the same mechanism as the signal. Besides, for the noise with dimensionless amplitudes comparable to or larger than one, additional noise components will be generated by frequency mixing due to the system nonlinearity.

Noise-induced increase in statistics improving output signal and contamination of the output by noise act in opposite directions and, at least partially, compensate each other. Clearly, interaction of noise with a thermally activated reaction modifies signal transfer, but can noise addition play a constructive role? Here, following our recent work^{3,27} we present a detailed analysis of this problem.

A. Signal and noise transfer—Adiabatic approximation

We limit ourselves to the adiabatic small-signal regime by assuming that the input voltage is a sum of a slow zero-mean Gaussian noise $V_N(t)$ and a slow small-amplitude sine-wave signal,

$$V(t) = V_N(t) + V_S \sin(2\pi f_S t), \tag{3}$$

where $V_S \ll 1/|\beta|$. The noise corner frequency, f_c , defining noise bandwidth, and the signal frequency, f_S , are assumed to be much smaller than all other characteristic frequencies in the system including the inverse pulse duration. In this case signal transduction properties can be described by the low-frequency part of the process power spectrum in the vicinity of f_S . A particular pulse shape is not important as it introduces a spectral “form-factor” that deviates from 1.0 only at high frequencies comparable or higher than the inverse pulse duration. At low frequencies the power spectral density of time-independent Poisson process with rate r is “white” and equals²⁹

$$S_i(f) = 2rQ^2, \tag{4}$$

where Q is an area under a single pulse. If output pulses represent electric current, then Q equals the total charge transferred through the circuit during a single pulse.

If the process rate is changing according to Eqs. (2) and (3), the low-frequency spectrum contains additional components reflecting the rate time behavior. Applied voltage will modulate pulse density in time introducing correlations in the pulse arrival times. The low-frequency power spectral density of such a doubly-stochastic Poisson process² can be written as

$$S_i(f) = 2Q^2 \langle r(V(t)) \rangle + 4(Qr(0))^2 \times \int_0^\infty \langle \exp(\beta V(t)) \exp(\beta V(t+\tau)) \rangle \cos(2\pi f\tau) d\tau. \tag{5}$$

The first term in the right-hand side of Eq. (5) stands for the component expected from a time-independent Poisson process [Eq. (4)] with a steady rate $\langle r(V(t)) \rangle$ increased in comparison to the initial rate $r(0)$ by applied noise because of system nonlinearity [Eq. (2)]. For Gaussian noise of r.m.s. amplitude σ and small signal, $V_S \ll \sigma$, this average is

$$\langle r(V(t)) \rangle = r(0) \exp((\beta\sigma)^2/2). \tag{6}$$

The second term in the right-hand side of Eq. (5) describes additional low-frequency spectral contributions from input signal and noise. Input noise not only increases the average process rate [Eq. (6)], but, together with the signal, it is also transduced to the system output by the mechanism illustrated in Figures 2 and 3. To calculate these contributions, we introduce a random vector $X \equiv \beta V(t)$, $Y \equiv \beta V(t)$ in order to be able to use Rice relations²⁹ for two-dimensional normal distributions. As a result, for the correlator under the integration sign in Eq. (5) we have

$$\langle \exp(\beta V(t)) \exp(\beta V(t+\tau)) \rangle = \exp((\beta\sigma)^2(1 + \rho(\tau))), \tag{7}$$

where $\rho(\tau)$ is the normalized autocorrelation function of the system input, $V(t)$, Eq. (3). In the current treatment we restrict ourselves to the input noise with a Lorentzian power spectrum,

$$S_N(f) = S_N(0)/(1 + (f/f_c)^2) = (2\sigma^2/\pi f_c)/(1 + (f/f_c)^2), \tag{8}$$

where $S_N(0)$ is the low-frequency power spectral density of the input noise and f_c is the corner frequency limiting noise bandwidth and defined through the single-pole filter relaxation time τ_F as $f_c = 1/2\pi\tau_F$. In this case the autocorrelation function is

$$\rho(\tau) = \exp(-\tau/\tau_F) + (V_S^2/2\sigma^2)\cos(2\pi f_S\tau), \tag{9}$$

and Eq. (5) becomes

$$S_i(f) = 2Q^2r(0)\exp\left(\frac{(\beta\sigma)^2}{2}\right) + \frac{2(Qr(0)\beta\sigma)^2}{\pi f_c} \exp((\beta\sigma)^2) \sum_1^\infty \frac{(\beta\sigma)^{2n-2}}{n!n} + \frac{(Qr(0)\beta V_S)^2}{2} \exp((\beta\sigma)^2) \delta(f-f_S). \tag{10}$$

The two first terms in the right-hand side of this expression describe a frequency-independent noise background at the system output. The first one accounts for the noise expected from a time-independent Poisson process with the pulse generation rate increased by a factor $\exp((\beta\sigma)^2/2)$ in comparison to the initial rate $r(0)$. This increase can be viewed as the input noise ‘‘rectification’’ by the system non-linearity. The second term represents the input noise transferred to the system output. It describes not only small-amplitude transduction (the case $\sigma \rightarrow 0$ would correspond to the sum in the second term converging to 1.0), but also the effects of frequency mixing for different spectral noise components. The last term shows the output signal. The addition of input noise increases signal (power) transduction coefficient by a factor $\exp((\beta\sigma)^2)$.

B. Output SNR and its dependence on noise parameters

The intensity of the output signal component obtained experimentally depends on the frequency resolution of the measuring device. This intensity is given by the prefactor of the delta-function in the last term of Eq. (10) divided by the device frequency resolution Δf_A . We calculate output signal-to-noise ratio, SNR, dividing this signal term by the sum of the first two:

$$SNR = \frac{(\beta V_S)^2 r(0)}{2\Delta f_A} \exp\left(\frac{(\beta\sigma)^2}{2}\right) / \left(2 + \frac{2r(0)}{\pi f_c} \exp\left(\frac{(\beta\sigma)^2}{2}\right) \sum_1^\infty \frac{(\beta\sigma)^{2n}}{n!n} \right). \tag{11}$$

It is seen that output SNR increases with the input signal amplitude and with an improvement of the measuring device spectral resolution (smaller Δf_A). Also, in the absence of any input noise ($\sigma = 0$, and the second term of the denominator

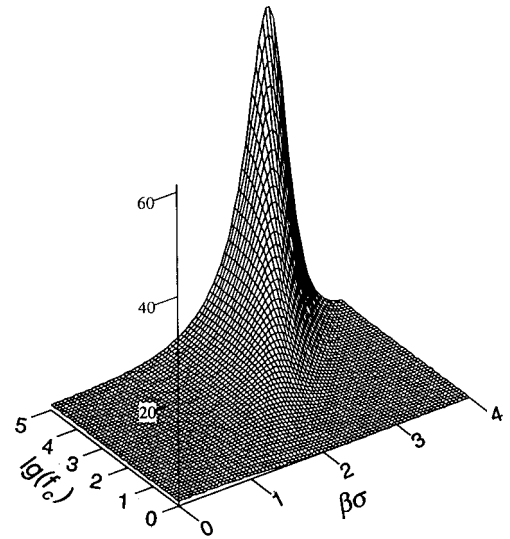


FIG. 4. Output signal quality, SNR, as a function of the input noise parameters: dimensionless intensity, $\beta\sigma$, and corner frequency f_c . It is seen that at sufficiently high corner frequencies (in comparison to the initial rate of the process, see the text) and proper noise intensities a significant improvement in the output signal quality is achieved. For the range of variables used here [$1 < \pi f_c/2r(0) < 10^5$ and $0 < \beta\sigma < 4$] the maximum SNR improvement reaches 61.4 times at $\pi f_c/2r(0) = 10^5$ and $\beta\sigma = 3.0$.

vanishes because of the sum that equals zero), the SNR is proportional to the process rate $r(0)$. These features of signal transduction are trivial; they could be expected from rather general considerations. What is not so obvious is the SNR dependence on the input noise parameters. The addition of noise modifies the simple dependence of output SNR on the process rate so that the relation $SNR \propto r(0)$ is no longer true.

The three-dimensional (3-D) plot in Figure 4 shows output SNR as a function of input noise reduced intensity, $\beta\sigma$, and its bandwidth, f_c . For convenience, the SNR calculated according to Eq. (11) is presented here (and in Figures 5–7) as a ratio to its value at $\sigma = 0$. The initial rate is taken equal to $\pi/2$. It is seen that the input noise with the properly chosen parameters can significantly increase output signal quality. There is an optimal combination of noise intensity and bandwidth; higher corner frequencies correspond to higher intensities.

This point is made clear by Figure 5 that shows output SNR in a semi-logarithmic scale as a function of the input noise intensity at different noise corner frequencies [or $\pi f_c/2r(0)$ ratios]. The data show that for the noise with a Lorentzian spectrum (single-pole passive filtering) an improvement in signal transduction quality is achieved only if $\pi f_c/2r(0) > 1$. Otherwise, noise addition only deteriorates the output signal.

For the input noise with a sharp spectral cut-off, the corresponding condition differs by a $2/\pi$ factor. Indeed, in this case the low-frequency spectral density of the input noise is σ^2/f_c . Considering only small noise amplitudes in order to discriminate between positive and negative noise influence (see Figure 5) we can substitute the second term in the right hand side of Eq. (10) with $H^2\sigma^2/f_c$ where H is the small-signal transduction coefficient (dimensionality A/V),

$$H^2 = (Qr(V_0)\beta)^2 \exp((\beta\sigma)^2). \tag{12}$$

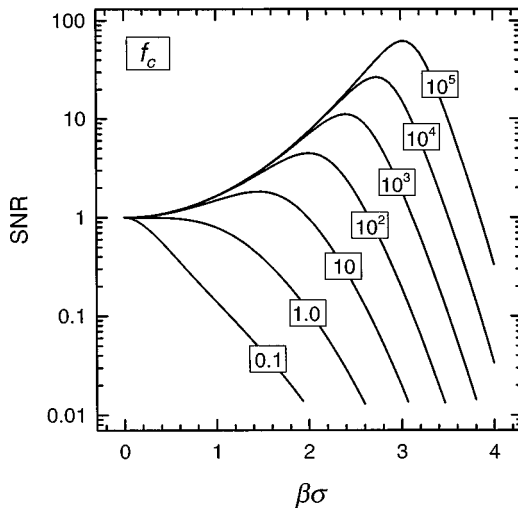


FIG. 5. Output SNR as a function of the input noise intensity at different $\pi f_c/2r(0)$ ratios. The addition of noise to the system input can either increase or decrease the output signal quality, depending on the ratio of the noise corner frequency, f_c , to the initial process rate, $r(0)$. For sufficiently high corner frequencies small intensity input noise always increases output SNR. Optimal noise intensity corresponding to the maximal output signal improvement grows with the $f_c/r(0)$ ratio.

Analysis of the resulting expression for the SNR gives the following condition for the stochastic resonance onset: $f_c/r(0) > 1$. For the constructive role of noise in signal transduction its bandwidth should be high enough. Input noise corner frequency should exceed the initial process rate. The higher their ratio, the greater is SNR improvement.

Figure 6 shows output SNR as a function of input noise corner frequency, f_c . It is seen that any amount of noise increases output SNR if f_c is high enough. At a fixed noise intensity, the SNR saturates with f_c to a σ -dependent value always exceeding 1.0.

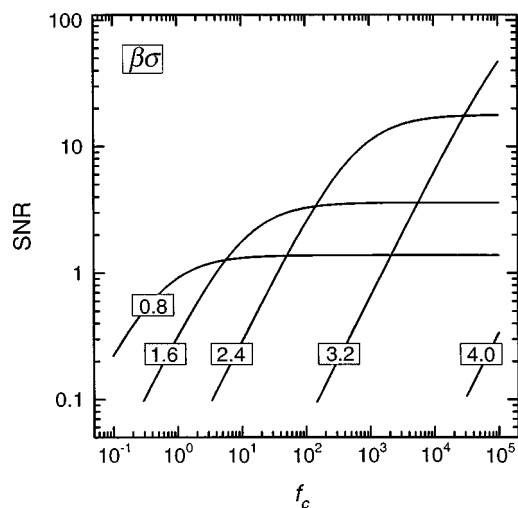


FIG. 6. Output SNR as a function of the noise corner frequency, f_c , at different input noise intensities, $\beta\sigma$. Input noise with sufficiently high corner frequencies always increases the output signal quality, but the effect of noise addition saturates with increasing f_c . The higher is noise intensity, the more pronounced is signal improvement at $f_c \rightarrow \infty$.

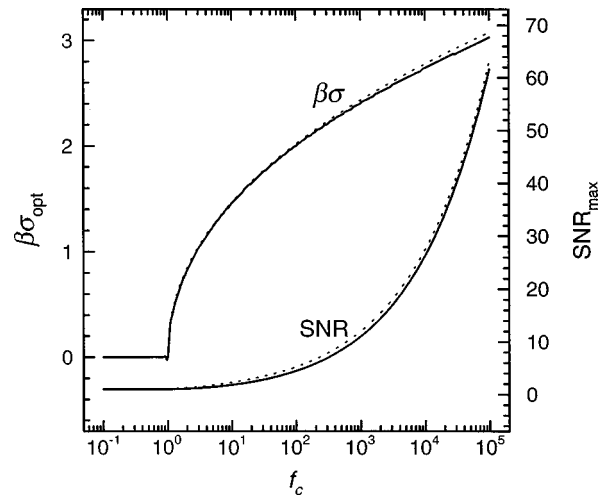


FIG. 7. Maximal output SNR (vertical axis on the right) and corresponding optimal noise intensity (vertical axis on the left) as functions of noise corner frequency, f_c . Significant SNR improvement requires high $f_c/r(0)$ ratios—the quality of signal transduction grows infinitely as the input noise becomes less and less correlated ($f_c \rightarrow \infty$). Dotted lines represent empirical relations useful for maximal SNR and optimal $\beta\sigma$ estimations (see the text).

The optimal input noise intensity and corresponding maximal output SNR are plotted in Figure 7. For simplicity, the initial rate is again taken equal to $\pi/2$. Analysis of Eq. (11) demonstrates that at $f_c/r(0)$ ratios smaller than 10^5 , the optimal noise intensity can be estimated as

$$\sigma_{opt} \cong \frac{1}{\beta} \sqrt{\ln \frac{\pi f_c}{2r(0)}} \tag{13}$$

The corresponding approximate relation for the maximal output SNR is

$$\text{SNR}_{max} \cong \sqrt[3]{\frac{\pi f_c}{2r(0)}} \tag{14}$$

For noise with a sharp spectral cut-off the $\pi/2$ factor should be omitted. Dotted lines along $\beta\sigma_{opt}$ and SNR_{max} curves represent $(\ln f_c)^{0.46}$ and $f_c^{0.36}$ plots, correspondingly.

C. Relationship between input and output SNR

To conclude our discussion of noise-facilitated signal transduction in thermally activated reactions we consider the input/output SNR issue. As we have shown above, a noise addition to the system input increases output signal and, if noise characteristics are properly adjusted (Figure 4), improves output signal quality in terms of SNR. Input noise most certainly plays a constructive role. A separate widely discussed question^{30–33} is the relationship between the input and output SNR of a stochastic resonator.

Our model permits a straightforward calculation of the output SNR vs the input SNR ratio. The input SNR for an ideal input signal, that is for a pure sine-wave, is the ratio of the spectral component of the input signal, $V_S^2/2\Delta f_A$, to the low-frequency spectrum of the added input noise, $S_N(0)$, that is given by Eq. (8). Then, the output SNR vs the input SNR ratio for an ideal signal, χ_{IS} , can be calculated as

$$\chi_{IS} = \frac{(\beta\sigma)^2 \exp\left(\frac{(\beta\sigma)^2}{2}\right)}{\frac{\pi f_c}{r(0)} + \exp\left(\frac{(\beta\sigma)^2}{2}\right) \sum_1^\infty \frac{(\beta\sigma)^{2n}}{n!n}} \quad (15)$$

This ratio is shown as a 3-D plot in Figure 8 as a function of $\beta\sigma$ and f_c values. The initial rate $r(0)$ is taken equal to 1. It is seen that the output SNR never exceeds the input SNR and approaches its value only for small noise amplitudes when corner frequency is low, $f_c \rightarrow 0$. A comparison of Figures 4 and 8 shows that the ranges of parameters that are optimal for stochastic resonance observation and conservation of input SNR do not overlap. Indeed, significant output SNR improvement is reached for large corner frequencies (Figure 4), while conservation of the input SNR requires the opposite condition (Figure 8).

It is easy to show that this contradiction is apparent and is completely related to the choice of ideal signal that is devoid of any practical interest. In the case of a sine-wave initially contaminated by the narrow-band noise with the power spectral density at the signal frequency N_S , the input SNR is

$$\text{SNR}_{\text{input}} = \frac{V_S^2/2\Delta f_A}{2\sigma^2/\pi f_c + N_S} \quad (16)$$

The output SNR vs the input SNR ratio for a noisy input signal, χ_{NS} , can be written in the form

$$\chi_{NS} = \frac{\left(\frac{2(\beta\sigma)^2}{\pi f_c} + \beta^2 N_S\right)}{\frac{2}{r(0)} \exp\left(-\frac{(\beta\sigma)^2}{2}\right) + \beta^2 N_S + \frac{2}{\pi f_c} \sum_1^\infty \frac{(\beta\sigma)^{2n}}{n!n}} \quad (17)$$

This function is illustrated in Figure 9 as a 3-D plot vs $\beta\sigma$ and f_c values. For simplicity, signal-contaminating noise spectral density is chosen to obey $\beta^2 N_S = 1$, and $r(0) = 1$. It is seen that independently of signal amplitude, input signal quality is nearly conserved (that is, χ_{NS} is close to one) if added noise corner frequencies are high enough and its in-

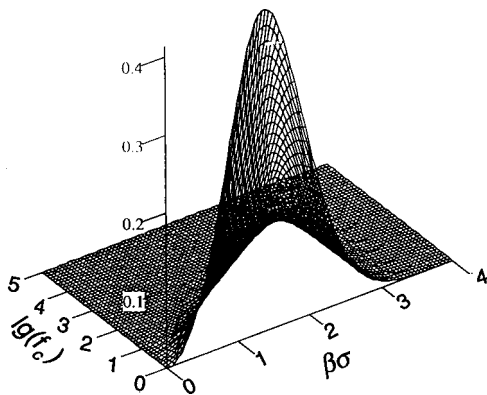


FIG. 8. The output SNR/ input SNR ratio for an ideal (noise-free) input signal as a function of the input noise parameters: dimensionless intensity, $\beta\sigma$, and corner frequency f_c . It is seen that in the whole range of variables used [$1 < \pi f_c/2r(0) < 10^5$ and $0 < \beta\sigma < 4$] the ratio stays well below 1.0. The maximum value of 0.41 is achieved at a noise intensity equal to 1.4.

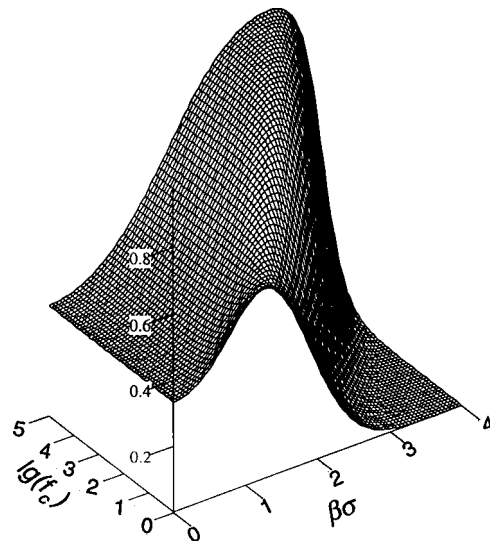


FIG. 9. The output SNR/ input SNR ratio for a real (noisy) input signal as a function of the input noise parameters. It is seen that in the practically interesting case of a signal with a finite noise background, the ratio approaches unity in the same range of the input noise parameters where significant improvement in the output SNR is obtained (compare to Figure 4). The addition of noise with the properly chosen parameters to the system input increases system performance virtually conserving SNR of the input signal.

tensity is properly adjusted. Importantly, the range of optimal parameters coincides now with that for stochastic resonance (Figure 4).

III. VOLTAGE-GATED ION CHANNELS AS THERMALLY ACTIVATED MOLECULAR REACTIONS

In electrophysiology, nonlinear properties of voltage-gated ion channels are usually characterized by the so-called ‘‘gating charge.’’²³ Gating charge describes the sensitivity of conformational dynamics of the channel open/closed transitions to trans-membrane electric fields. In the simplest two-state case, a channel fluctuates between its open and closed conformations with probabilities P_O and P_C , correspondingly. We assume that the conformational transition between these two states moves n electron charges from one membrane surface to the other. If sensitivity of channel conformational dynamics to an electric field can be entirely attributed to the movement of these charges, conformational balance is described by the following relation widely used in the physiology of excitable cells:^{4,23}

$$\frac{P_O}{P_O + P_C} = P_O = \frac{1}{1 + \exp((w - neV)/kT)} \quad (18)$$

Here, w is conformation energy increase in the channel closed-to-open transition. Equation (18) is the well-known Boltzmann equation applied to conformational statistics. It highlights the equilibrium nature of ion channel transitions between different states.

If the probability to find the channel in the open state is small, that is $P_O \ll 1$, Eq. (18) becomes

$$P_O \cong \exp\left(\frac{-w}{kT}\right) \exp\left(\frac{neV}{kT}\right) \quad (19)$$

Another parameter widely used in the ion channel description is a mean life-time of the open state, τ_o . For $P_o \ll 1$, this parameter is related to total rate of a single channel opening, $r_s(V)$, as $r_s(V)\tau_o = P_o$. Using this relation and considering N independent channels in parallel, for the generation rate of transmembrane current pulses we have

$$r(V) \cong \frac{N}{\tau_o} \exp\left(\frac{-w}{kT}\right) \exp\left(\frac{neV}{kT}\right). \quad (20)$$

For sufficiently small open state probabilities, the correlation between moments of successive openings of the same channel are negligible. Then, the resulting train of current pulses will represent a time-dependent Poisson wave with the generation rate obeying Eq. (2) where

$$r(0) = \frac{N}{\tau_o} \exp\left(\frac{-w}{kT}\right) \quad (21)$$

and

$$\beta = \frac{ne}{kT}. \quad (22)$$

Thus, conformational dynamics of voltage-gated ion channels of biological membranes can be viewed as thermally activated reactions controlled by voltage-dependent activation barrier (Figure 1) with parameters described by Eqs. (2), (21), and (22).

Gating charge is usually determined in experiments with depolarizing voltage steps.⁴ It is calculated from the dependence of the number of simultaneously open channels on the applied transmembrane potential. The so-called "limiting equivalent sensitivities" are voltage differences corresponding to an e -fold increase in the open channel population that are measured in the steepest region of this dependence. According to Eq. (19), limiting equivalent sensitivity of 3.9 mV for the sodium and 4.8 mV for the potassium channel recalculates to about 6 and 4.5 electron charges linked to gating.⁴

The mechanism of voltage gating is not fully understood. Because of this, the gating charge introduced through Eqs. (18) and (19) is mostly a convenient empirical parameter. The actual number of elementary charges responding to the external field is probably much larger. Indeed, if the conformational transition between open and closed states moves the charges only half-way through the membrane, their number has to be doubled to account for the same sensitivity. Nevertheless, usefulness of the gating charge concept goes beyond empirical convenience; it introduces a simple physical picture for a complex biological phenomenon.

Conformational dynamics of voltage-gated ion channels are studied by many different approaches; most informative ones designed to observe currents through a single channel. With patch-clamp techniques³⁴ a small patch of a cell membrane is isolated by using special micropipettes. In ion channel reconstitution techniques,³⁵ ion channel forming proteins are first purified and then reinserted into artificial planar lipid membranes. Both approaches allow recording of ionic current from a single ion channel—a single protein molecule

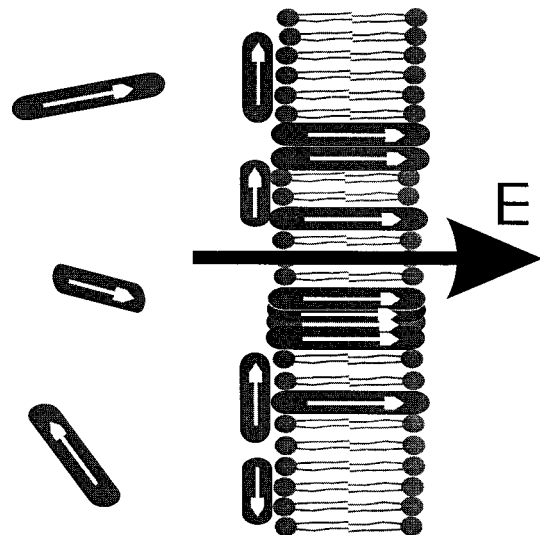


FIG. 10. An illustration of a possible mechanism of alamethicin channel voltage sensitivity. The electric field applied to the membrane interacts with polypeptide molecules via their dipole moment. Equilibrium between populations of alamethicin molecules adsorbed to the membrane surface and traversing the membrane is voltage-dependent. Stronger fields increase the number of trans-membrane oriented molecules. Trans-oriented molecules aggregate into ion-conducting clusters that are seen as "bursts" in ion current through the membrane (Figure 11).

embedded in a lipid bilayer—with time-resolved current "steps" of the channel transitions between different conductive states.

General physical mechanisms underlying voltage sensitivity of ion channels can also be studied with model polypeptides. One of the most widely used is alamethicin, a 20-amino acid peptide of relatively rigid, rod-like structure.^{36–38} In lipid bilayers it forms ion channels whose conformational equilibrium is voltage-dependent with the equivalent voltage sensitivity that is close to that of sodium channels of excitable membranes.³⁹ There are several hypotheses for the voltage sensitivity of alamethicin-induced conductance (see a review³⁸). Most of them rely on the interactions between a transmembrane electric field and a 75 Debye dipole moment of the alamethicin molecule.

A possible mechanism is illustrated in Figure 10. The interaction of the electric field with the peptide dipole moment increases the number of peptide molecules with a trans-membrane orientation. The trans-oriented molecules then aggregate into conducting clusters of different sizes. The equilibrium between populations of molecules bound to the membrane surface and molecules in the transmembrane orientation is voltage-dependent; the equilibrium between monomers and aggregates is not. The average number of simultaneously open channels grows exponentially with voltage increasing e -times every 4.1 ± 0.6 mV (for membranes made of diphytanoyl phosphatidylcholine²⁷) over a significant range of field strengths. The equivalent gating charge is 5 to 7 electron charges. The absence of saturation, interpreted within a framework of the model shown in Figure 10, means that surface-bound population dominates at all voltages. Formal interpretation through Eq. (18) leads to a con-

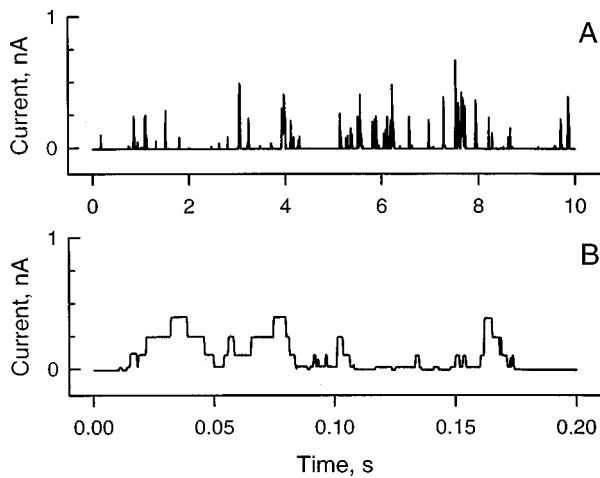


FIG. 11. Single alamethicin ion channels are seen as spontaneous bursts in transmembrane current. A higher resolution recording (B) shows the fine structure of a single burst, explaining pulse height variability in a lower resolution recording (A). Holding potential of +140 mV (positive from the side of polypeptide addition) and a 2.5 mV (r.m.s.) sine-wave signal of 0.5 Hz frequency are applied to the membrane bathed by 1 M NaCl aqueous solution. Output signal is filtered by a low-pass Bessel filter with 150 Hz (A) or 5,000 Hz (B) corner frequencies.

clusion that conformational energy w is high, of the order of $10 kT$ or more.

Alamethicin channels are seen as spontaneous “bursts” of the membrane ion current. Two representative current traces with the time resolution differing by a factor of 50 are shown in Figure 11. Trace A demonstrates randomly arriving current pulses with varying amplitude. Higher resolution recording (B) explains this variability by displaying multiple substates within a single current burst that correspond to alamethicin clusters of different size. A channel is thermally activated into its lowest conductive substate, undergoes several random transitions between different adjacent substates, and, eventually, is deactivated. While the probability for a channel to open is highly voltage-dependent, its average stochastic behavior in the open state is rather voltage-insensitive.

A small sine-wave signal added to the membrane holding potential of 140 mV introduces periodicity in the channel generation rate. Hardly perceptible by eye, this periodicity is easily detected by spectral analysis. The amplitude of the signal spectral component of the alamethicin current pulses significantly exceeds the amplitude expected from a passive linear circuit of the same conductance.²⁷ Their ratio (in power spectral density units) was shown to obey the following relation:

$$\alpha^2 = (1 + neV_0/kT)^2, \quad (23)$$

where V_0 is the holding potential supporting a particular average number of open ion channels. This relation can be derived from our theoretical analysis of signal transduction in thermally activated reactions. Indeed, the output signal of a passive linear circuit representing ion channels with their voltage sensitivity switched off ($n=0$) can be written as a product of signal voltage by the average channel-induced conductance, $r(V_0)h\tau_0$, where h is conductance of a single

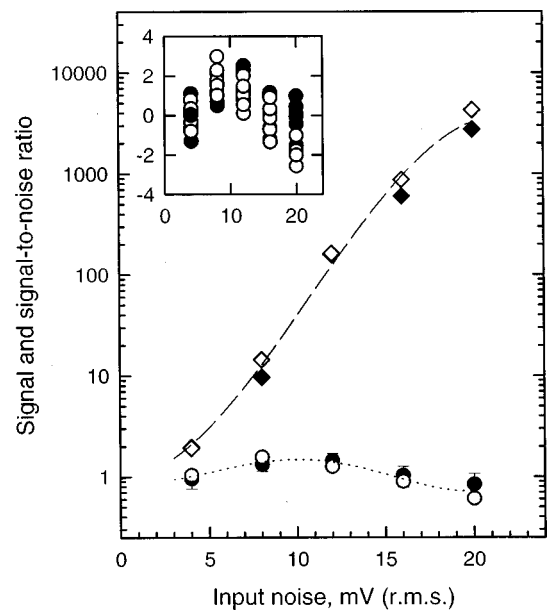


FIG. 12. The addition of noise to the transmembrane voltage increases output signal power (diamonds) and, at optimal noise intensity, output SNR (circles).²⁷ Sine-wave signals of constant amplitude (5 mV r.m.s.) and frequencies (0.2 Hz, filled symbols; 0.5 Hz, open symbols) were mixed with different amounts of noise and added to a holding potential of +130 mV. The inset shows statistics of SNR measurements.

channel. From the other hand, the output signal of a parallel array of voltage-sensitive channels equals a product of signal voltage by the sum $r(V_0)h\tau_0 + H$, where H is defined by Eq. (12). Taking into account that Q in Eq. (12) stands for the total average charge carried through the channel current pulse, that is $Q = V_0h\tau_0$, and considering the case of zero input noise, $\sigma=0$, we arrive at Eq. (23).

We have studied alamethicin channels from the point of view of electrical signal transduction in the presence of external input noise.²⁷ Output signal amplitude and output SNR were measured as functions of input noise intensity. The results shown in Figure 12 demonstrate a pronounced noise-induced increase in the output signal (diamonds). Output SNR (circles) exhibits a small but statistically significant maximum of around 10 mV (r.m.s.) noise. Two signal frequencies (0.2 Hz, open symbols, and 0.5 Hz, filled symbols), both smaller than the voltage-sensitivity cut-off frequency of 2 Hz, were used.

Theoretical analysis of signal transduction in thermally activated reactions presented in the previous section allows us to calculate optimal noise intensity and corresponding improvement in the output signal quality. Using Eqs. (13) and (14) with β defined by Eq. (22) and the following parameters²⁷—initial channel generation rate, $r(0) = 0.3 \text{ s}^{-1}$; input noise corner frequency, $f_c = 2 \text{ Hz}$, channel gating charge, $ne = 5-7$ electron charges—we obtain $\sigma_{opt} \approx 6-8 \text{ mV}$ and $\text{SNR}_{max} \approx 3-4 \text{ dB}$. These values are in surprisingly good agreement with the experimental results plotted in Figure 12. Indeed, the theory formulation included several assumptions that hardly hold in our experiment. First, identical pulses that do not show any spread in amplitudes or durations were considered. Second, the theory was formulated for small signals $V_S \ll kT$ and $V_S \ll \sigma$. Third, possible

correlations between different pulses were altogether neglected.⁴⁰

IV. CONCLUSIONS

The agreement between theoretical predictions and experiment demonstrates that our treatment of signal transfer in thermally activated reactions is an adequate description of external noise interaction with voltage-gated ion channels. It provides an understanding of physical mechanisms involved in noise-facilitated signal transduction at the molecular level and offers a quantitative tool for its analysis.

We show that stochastic resonance is an inherent feature of a time-dependent Poisson process with the rate that is exponentially sensitive to an external parameter. We describe the following features of signal transfer:

- Threshold-free response — the transfer of small signals with a transduction coefficient that is independent of the signal amplitude;
- noise-facilitated signal transduction — an increase in the output signal amplitude by the noise addition to the system input;
- noise-induced improvement of the output signal quality — an increase in the output signal SNR by input noise with a properly chosen parameters.

We also show that for realistic signals, that is for signals with a finite initial SNR, the addition of noise to the system input can improve system performance essentially conserving SNR of the input signal.

ACKNOWLEDGMENTS

We thank V. Adrian Parsegian for many enlightening discussions. We appreciate consultations with George Weiss and Ralph Nossal, and are grateful to Donald C. Rau for comments on the manuscript.

- ¹K. Wiesenfeld and F. Moss, "Stochastic resonance and the benefits of noise: from ice ages to crayfish and SQUIDS," *Nature* **373**, 33–36 (1995).
- ²D. R. Cox and P. A. W. Lewis, *The Statistical Analysis of Series of Events*, Methuen, London, 1966.
- ³S. M. Bezikov and I. Vodyanoy, "Stochastic resonance in non-dynamical systems without response thresholds," *Nature* **385**, 319–321 (1997).
- ⁴A. L. Hodgkin and A. F. Huxley, "A quantitative description of membrane current and its application to conduction and excitation in nerve," *J. Physiol. (London)* **117**, 500–544 (1952).
- ⁵P. Hanggi, P. Talkner, and M. Borkovec, "Reaction-rate theory: fifty years after Kramers," *Rev. Mod. Phys.* **62**, 251–342 (1990).
- ⁶A. M. Berezhkovskii, A. N. Drozdov, and V. Yu. Zitserman, "Kramers kinetics: present state," *Russ. J. Phys. Chem.* **62**, 1353–1361 (1988).
- ⁷A. R. Bulsara, S. B. Lowen, and C. D. Rees, "Cooperative behavior in the periodically modulated Wiener process: Noise-induced complexity in a model neuron," *Phys. Rev. E* **49**, 4989–5000 (1994).
- ⁸X. Pei, L. Wilkens, and F. Moss, "Noise-mediated spike timing precision from aperiodic stimuli in an array of Hodgkin-Huxley-type neurons," *Phys. Rev. Lett.* **77**, 4679–4682 (1996).
- ⁹F. Chapeau-Blondeau, X. Godivier, and N. Chambet, "Stochastic resonance in a neuron model that transmits spike trains," *Phys. Rev. E* **53**, 1273–1275 (1996).
- ¹⁰A. Longtin, "Autonomous stochastic resonance in bursting neurons," *Phys. Rev. E* **55**, 868–876 (1997).
- ¹¹H. E. Plesser and S. Tanaka, "Stochastic resonance in a model neuron with reset," *Phys. Lett. A* **225**, 228–234 (1997).
- ¹²B. J. Gluckman, T. I. Netoff, E. J. Neel, W. L. Ditto, M. L. Spano, and S.

- J. Schiff, "Stochastic resonance in a neuronal network from mammalian brain," *Phys. Rev. Lett.* **77**, 4098–4101 (1996).
- ¹³D. R. Chialvo, A. Longtin, and J. Mullergerking, "Stochastic resonance in models of neuronal ensembles," *Phys. Rev. E* **55**, 1798–1808 (1997).
- ¹⁴R. P. Morse and E. F. Evans, "Enhancement of vowel coding for cochlear implants by addition of noise," *Nat. Med.* **2**, 928–932 (1996).
- ¹⁵F. Moss, F. Chiou-Tan, and R. Klinke, "Will there be noise in their ears?," *Nat. Med.* **2**, 860–862 (1996).
- ¹⁶J. J. Collins, T. T. Imhoff, and P. Grigg, "Noise-enhanced information transmission in rat SA1 cutaneous mechanoreceptors via aperiodic stochastic resonance," *J. Neurophysiol.* **76**, 642–645 (1996).
- ¹⁷J. L. Douglass, L. Wilkens, E. Pantazelou, and F. Moss, "Noise enhancement of information transfer in crayfish mechanoreceptors by stochastic resonance," *Nature* **365**, 337–340 (1993).
- ¹⁸J. E. Levin and J. P. Miller, "Broadband neural encoding in the cricket cercal sensory system is enhanced by stochastic resonance," *Nature* **380**, 165–168 (1996).
- ¹⁹P. Cordo, T. Inglis, S. Verschuere, J. J. Collins, D. Merfeld, S. Rosenblum, S. Buckley, and F. Moss, "Noise in human muscle spindles," *Nature* **383**, 769–770 (1996).
- ²⁰J. J. Collins, T. T. Imhoff, and P. Grigg, "Noise-enhanced tactile sensation," *Nature* **383**, 770 (1996).
- ²¹F. Y. Chiou-Tan, K. Magee, L. Robinson, M. Nelson, S. Tuel, T. Krouskop, and F. Moss, "Enhancement of sub-threshold sensory nerve action potentials during muscle tension mediated noise," *J. Bifurc. Chaos* **6**, 1389–1396 (1996).
- ²²E. Simonoto, M. Riani, C. Seife, M. Roberts, J. Twitty, and F. Moss, "Visual perception of stochastic resonance," *Phys. Rev. Lett.* **78**, 1186–1189 (1997).
- ²³B. Hille, *Ionic Channels of Excitable Membranes* (Sinauer, Sunderland, MA, 1992).
- ²⁴B. Alberts, D. Bray, J. Lewis, M. Raff, K. Roberts, and J. D. Watson, *Molecular Biology of the Cell* (Garland, New York, 1994).
- ²⁵J. Lu and H. M. Fishman, "Interaction of apical and basal membrane ion channels underlies electroreception in ampullary epithelia of skates," *Biophys. J.* **67**, 1525–1533 (1994).
- ²⁶S. M. Bezikov and I. Vodyanoy, "Noise-induced enhancement of signal transduction across voltage-dependent ion channels," *Nature* **378**, 362–364 (1995).
- ²⁷S. M. Bezikov and I. Vodyanoy, "Signal transduction across alamethicin ion channels in the presence of noise," *Biophys. J.* **73**, 2456–2464 (1997).
- ²⁸J. S. Bendat and A. G. Piersol, *Random Data: Analysis and Measurement Procedures* (Wiley, New York, 1986).
- ²⁹S. O. Rice, "Mathematical analysis of random noise," in *Selected Papers on Noise and Stochastic Processes*, edited by N. Wax (Dover, New York, 1954), pp. 133–294.
- ³⁰M. DeWeese and W. Bialek, "Information flow in sensory neurons," *Nuovo Cimento D* **17**, 733–741 (1995).
- ³¹M. I. Dykman, D. G. Luchinsky, R. Manella, P. V. E. McClintock, N. D. Stein, and N. G. Stocks, "Stochastic resonance in perspective," *Nuovo Cimento D* **17**, 661–683 (1995).
- ³²K. Loerincz, Z. Gingl, and L. B. Kiss, "A stochastic resonator is able to greatly improve signal-to-noise ratio," *Phys. Lett. A* **224**, 63–67 (1996).
- ³³L. B. Kiss, "Possible breakthrough: significant improvement of signal to noise ratio by stochastic resonance," in *Chaotic, Fractal, and Nonlinear Signal Processing*, edited by R. Katz (AIP Press, New York, 1996), pp. 382–396.
- ³⁴B. Sakmann and E. Neher, *Single-Channel Recording* (Plenum, New York, 1995).
- ³⁵C. Miller, *Ion Channel Reconstitution* (Plenum, New York, 1986).
- ³⁶M. S. P. Sansom, "The biophysics of peptide models of ion channels," *Prog. Biophys. Mol. Biol.* **55**, 139–235 (1991).
- ³⁷G. A. Woolley and B. A. Wallace, "Model ion channels: gramicidin and alamethicin," *J. Membr. Biol.* **129**, 109–136 (1992).
- ³⁸D. S. Cafiso, "Alamethicin: A peptide model for voltage gating and protein-membrane interactions," *Annu. Rev. Biophys. Biomol. Struct.* **23**, 141–165 (1994).
- ³⁹J. E. Hall, I. Vodyanoy, T. M. Balasubramanian, and G. R. Marshall, "Alamethicin. A rich model for channel behavior," *Biophys. J.* **45**, 233–247 (1984).
- ⁴⁰While this assumption definitely holds for small generation rates (small ion channel densities), it may be violated at high generation rates. Auto-correlation analysis of alamethicin channel currents at high channel den-

sities shows a conductance-dependent increase in correlation times [H.-A. Kolb and G. Boheim, "Analysis of the multipore system of alamethicin in a lipid membrane. II. Autocorrelation analysis and power spectral density," *J. Membrane Biol.* **38**, 151–191 (1978)]. It means that high input

noise intensities increasing the average channel generation rate by orders of magnitude, can change a number of system parameters such as the mean pulse duration and the characteristic cut-off frequency of channel voltage sensitivity.